GEOPHYSICS, VOL. 77, NO. 6 (NOVEMBER-DECEMBER 2012); P. N17–N24, 6 FIGS.
10.1190/GEO2011-0214.1

AVO inversion and poroelasticity with P- and S-wave moduli

Zhaoyun Zong[1], Xingyao Yin[1], and Guochen Wu[1]

ABSTRACT

The fluid term in the Biot-Gassmann equation plays an important role in reservoir fluid discrimination. The density term imbedded in the fluid term, however, is difficult to estimate because it is less sensitive to seismic amplitude variations. We combined poroelasticity theory, amplitude variation with offset (AVO) inversion, and identification of P- and S-wave moduli to present a stable and physically meaningful method to estimate the fluid term, with no need for density information from prestack seismic data. We used poroelasticity theory to express the fluid term as a function of P- and S-wave moduli. The use of P- and S-wave moduli made the derivation physically meaningful and natural. Then we derived an AVO approximation in terms of these moduli, which can then be directly inverted from seismic data. Furthermore, this practical and robust AVO-inversion technique was developed in a Bayesian framework. The objective was to obtain the maximum a posteriori solution for the P-wave modulus, S-wave modulus, and density. Gaussian and Cauchy distributions were used for the likelihood and a priori probability distributions, respectively. The introduction of a low-frequency constraint and statistical probability information to the objective function rendered the inversion more stable and less sensitive to the initial model. Tests on synthetic data showed that all the parameters can be estimated well when no noise is present and the estimated P- and S-wave moduli were still reasonable with moderate noise and rather smooth initial model parameters. A test on a real data set showed that the estimated fluid term was in good agreement with the results of drilling.

INTRODUCTION

Fluid discrimination is an important task in seismic exploration and reservoir description. The development of methods to obtain various fluid factors from prestack seismic data has pushed the rapid development of technology for reservoir forecasting and fluid discrimination (Smith and Gidlow, 2000; Quakenbush et al., 2006). Smith and Gidlow (1987) initially propose estimating the fluid factor and a pseudo Poisson ratio for lithology and fluid discrimination, based on a weighted stack method that used prestack seismic data. Goodway et al. (1997) propose lambda-mu-rho (LMR) technology for fluid discrimination, but it has some limits for practical reservoirs in porous media.

Poroelasticity theories that Biot (1941, 1956) and Gassmann (1951) present serve as rigorous foundations and useful tools for modeling physical rock-fluid interaction in situ and for fluid discrimination in exploration geophysics. Russell et al. (2003) use these theories and derive the fluid component (ρf), which is the combination of P-wave impedance, S-wave impedance, and a constant. They generalize the Goodway et al. (1997) amplitude variation with offset (AVO) approximate equation by incorporating the dry and saturated properties of the in-situ reservoir rock into the expression for the P-wave velocity. In contrast to LMR technology, the introduction of poroelasticity theory makes fluid discrimination more applicable, at least in theory. We will focus on the extraction of the fluid term f, which is the real factor that reflects the influence of fluid in porous rock as Russell et al. (2011) discuss. A brief introduction of these items is given in the next section, and we show there how these equations can be derived and reparameterized with the P-wave modulus, S-wave modulus, and dry velocity ratio, in a direct way that yields a meaningful and natural description.

The Zoeppritz equation (Zoeppritz, 1919) is the fundamental mathematical formula for the amplitudes of reflected and transmitted plane waves when an incident P-wave strikes an elastic boundary. Although it gives precise values of the amplitudes of the reflected and transmitted plane waves, the difficulty in understanding the effects of parameter changes on the seismic amplitudes

Manuscript received by the Editor 17 June 2011; revised manuscript received 17 June 2012; published online 27 September 2012; corrected version published online 21 November 2012.
[1]China University of Petroleum, Qingdao, Shandong, China. E-mail: zhaoyunzong@yahoo.com; xyyin@upc.edu.cn; guochenwu@upc.edu.cn.

and the unstable solution resulting from its intrinsic nonlinearity make it less practical than are linearized approximations to it. The linearized approximation to the Zoeppritz equations is the basis of AVO analysis and prestack inversion (Ikelle, 1995; Buland and Omre, 2003; Yin et al., 2008). A summary of different parameterized, linearized approximations is given by Russell et al. (2011), and we will show how some of these approximation equations compare with our novel approximation equation in terms of P-wave modulus, S-wave modulus, and density.

AVO inversion is a well-established seismic exploration methodology used to predict the earth's elastic parameters and rock and fluid properties based on a knowledge of elastic wave behavior and a set of geophysical measurements. Smith and Gidlow (1987) are the first to develop a P- and S-wave velocity reflectivity inversion method based on P-wave AVO variation. They also show success with a computationally simpler procedure of least-squares fitting of a weighted stack of the traces in a CMP gather. Additionally, considerable work has been carried out on AVO inversion (Buland and Landro, 1995; Simmons and Backus, 1996; Beretta et al., 2002; Downton and Ursenbach, 2006; Karimi et al., 2010). However, the three-parameter AVO-inversion problem is ill posed and noise levels may force the imposition of constraints to obtain stable and rational inversion results. Smith and Gidlow (1987) constrain density with Gardner's rule. Downton (2005) constrain three-parameter AVO inversion with probabilistic constraints on local geology, and he also estimates reliable density reflectivity, considering normal-moveout stretch and offset-dependent tuning. Jin et al. (2000) use singular value decomposition to stabilize the linearized P-SV reflection equations and to obtain reasonable results for synthetic and field data. Yin et al. (2008) add point constraints to enhance inversion stability. On the basis of previous studies, our current study proposes and implements a practical AVO inversion method, based on a novel AVO approximate equation. Gaussian and Cauchy distributions are used for the likelihood and a priori probability distributions, respectively. Because this results in weak nonlinear solutions, the iteratively reweighted least-squares (IRLS) method is applied for the optimization problem. We impose the low-frequency information constraint, from well logging, onto the objective function; meanwhile, that low-frequency information is also used to calculate the covariance matrix for each trace to improve the decorrelation for the parameters to be inverted. We end with model and real data case studies that illustrate the method.

POROELASTICITY THEORY WITH P- AND S-WAVE MODULI

Poroelasticity theories Biot (1941, 1956) and Gassmann (1951) present are the most robust and frequently implemented way to express the P- and S-wave velocities of porous rocks in terms of different kinds of elastic moduli. Biot (1941) and Gassmann (1951) use either the Lamé parameters (λ and μ), or the bulk modulus (k) and shear modulus (μ) to express the P- and S-wave velocities in porous, saturated rocks. These two kinds of approaches lead to the same result as shown by Garat et al. (1990). Russell et al. (2003) use these poroelasticity theories to generalize the Goodway et al. (1997) formulation, by incorporating dry and saturated properties of the in-situ reservoir rock into the expression for the P-wave velocity. Meanwhile, they establish a relationship between the fluid component and the P- and S-wave impedances of the in-situ reservoir rock, which could be inverted or extracted from prestack seismic data. A constant c is hypothesized to be the ratio of the dry-skeleton term and the dry-rock shear modulus to extract the fluid component ρf. Here, we focus on the fluid term f, which reflects the influence of fluid composition as Russell et al. (2011) discuss.

In fact, the Lamé parameter λ applied to express P-wave velocity in isotropic, elastic nonporous, or porous media has no physical interpretation, but it serves to simplify the stiffness matrix in Hooke's law (Mavko et al., 1998). We will follow the derivation of Biot (1941), but with more meaningful elastic moduli, namely, a P-wave modulus and an S-wave modulus, to reopen the question of poroelasticity.

First, the P- and S-wave velocity in isotropic, elastic nonporous media can be rewritten as

$$V_{\mathrm{P}} = \sqrt{\frac{M}{\rho}}, \qquad V_{\mathrm{S}} = \sqrt{\frac{\mu}{\rho}}, \tag{1}$$

where V_{P} is the P-wave velocity, V_{S} is the S-wave velocity, ρ is the density, M is the P-wave modulus defined as the ratio of axial stress to axial strain in a uniaxial-strain state, and μ is the S-wave modulus defined as the ratio of shear stress to the shear strain (Mavko et al., 1998).

For porous, saturated rocks, we also express the P- and S-wave velocity in terms of P- and S-wave moduli. The relationship for the P-wave modulus is shown as

$$M_{\mathrm{sat}} = M_{\mathrm{dry}} + \beta^2 M_p, \tag{2}$$

where M_{sat} is the P-wave modulus for the fluid-saturated rock, M_{dry} is the P-wave modulus for the dry frame, β is the Biot coefficient expressing the ratio of the volume change in the fluid to the volume change in the formation when hydraulic or pore pressure is constant, and M_p is the modulus representing the pressure needed to force fluid into the formation without changing the volume.

For the corresponding S-wave modulus in porous, saturated rocks, we have

$$\mu_{\mathrm{sat}} = \mu_{\mathrm{dry}}, \tag{3}$$

where μ_{sat} is the S-wave modulus for the fluid-saturated rock, and μ_{dry} is the S-wave modulus for the dry frame. Thus, the shear modulus is unaffected by the pore fluid.

Then, the P- and S-wave velocities in porous, saturated rocks may be rewritten as

$$(V_{\mathrm{P}})_{\mathrm{sat}} = \sqrt{\frac{M_{\mathrm{dry}} + \beta^2 M_p}{\rho_{\mathrm{sat}}}}, \tag{4}$$

$$(V_{\mathrm{S}})_{\mathrm{sat}} = \sqrt{\frac{\mu_{\mathrm{sat}}}{\rho_{\mathrm{sat}}}} = \sqrt{\frac{\mu_{\mathrm{dry}}}{\rho_{\mathrm{sat}}}}, \tag{5}$$

and

$$\rho_{\mathrm{sat}} = \rho_m(1-\phi) + \rho_w S_w \phi + \rho_h (1 - S_w)\phi, \tag{6}$$

where ρ_{sat} is the total density value, ρ_m is the density of the rock matrix if it were nonporous, ρ_w is the density of the water (brine), ρ_h is the density of the hydrocarbon, ϕ is the porosity of the rock, and S_w is the water saturation. M_p can be expressed as in Gassmann (1951), but it is not discussed here because it is not our focus.

Finally, when $\beta^2 M_p$ is defined as f, equation 2 becomes

$$f = M_{sat} - M_{dry}, \tag{7}$$

while

$$M_{dry} = \rho_{dry} \times (V_P)^2_{dry} = \left(\frac{V_P}{V_S}\right)^2_{dry} \times \rho_{dry} \times (V_S)^2_{dry} = \left(\frac{V_P}{V_S}\right)^2_{dry} \times \mu_{dry}. \tag{8}$$

With equations 3, 5, 7, and 8, it is easy to get

$$f = M_{sat} - \left(\frac{V_P}{V_S}\right)^2_{dry} \times \mu_{dry} = M_{sat} - \left(\frac{V_P}{V_S}\right)^2_{dry} \times \mu_{sat}. \tag{9}$$

From equation 9, we can estimate the mixed fluid/rock term f directly, with P- and S-wave moduli that can be inverted from prestack seismic data with the novel AVO approximation equations that we discuss later. The whole inferential process is meaningful and natural, and for a target reservoir, $(V_P/V_S)^2_{dry}$ can be estimated according to the discussion as given by Russell (2003), and still, the value of $(V_P/V_S)^2_{dry}$ can vary with different rock background at different depths in the field data, according to well-log interpretation.

AVO APPROXIMATION EQUATION WITH P- AND S-WAVE MODULI AND DENSITY

To describe a perfectly elastic isotropic earth medium, a combination of three parameters is needed. To estimate from seismic data, the fluid term f according to equation 9, we derive a novel linearized approximation using P- and S-wave moduli and density.

Under the assumption that two solid half-spaces are welded at an elastic interface and that only small relative changes in elastic parameters occur across the boundary, the P-wave reflection coefficient in terms of changes in P-wave, S-wave, and density can be expressed as in Aki and Richards (1980):

$$R(\theta) = \frac{1}{2}\left(1 - 4\left(\frac{V_S}{V_P}\right)^2_{sat} \sin^2\theta\right)\frac{\Delta\rho}{\rho} + \frac{\sec^2\theta}{2}\frac{\Delta V_P}{V_P} - 4\left(\frac{V_S}{V_P}\right)^2 \sin^2\theta \frac{\Delta V_S}{V_S}, \tag{10}$$

where θ is the incident angle, $\Delta V_P/V_P$ is the P-wave velocity reflectivity, $\Delta V_S/V_S$ is the S-wave velocity reflectivity, $\Delta\rho/\rho$ is the density reflectivity, and they can be expressed as

$$\frac{\Delta V_P}{V_P} = \frac{2(V_{P1} - V_{P2})}{(V_{P1} + V_{P2})}, \tag{11}$$

$$\frac{\Delta V_S}{V_S} = \frac{2(V_{S1} - V_{S2})}{(V_{S1} + V_{S2})}, \tag{12}$$

$$\frac{\Delta\rho}{\rho} = \frac{2(\rho_1 - \rho_2)}{(\rho_1 + \rho_2)}, \tag{13}$$

where $V_{P1}, V_{P2,} V_{P1}, V_{P2,} \rho_1, \rho_2$ are the related parameters in the media touching at the reflector.

With the relationships between the P-wave modulus reflectivity, S-wave modulus reflectivity, P-wave velocity, S-wave velocity, and density reflectivity, as shown below

$$\frac{\Delta V_P}{V_P} = \frac{1}{2}\left(\frac{\Delta M}{M} - \frac{\Delta\rho}{\rho}\right), \tag{14}$$

$$\frac{\Delta V_S}{V_S} = \frac{1}{2}\left(\frac{\Delta\mu}{\mu} - \frac{\Delta\rho}{\rho}\right) \tag{15}$$

we derived a new approximation equation in terms of P- and S-wave moduli

$$R(\theta) = \frac{1}{4}\sec^2\theta\frac{\Delta M}{M} - 2\left(\frac{V_S}{V_P}\right)^2_{sat} \sin^2\theta\frac{\Delta\mu}{\mu} + \left(\frac{1}{2} - \frac{1}{4}\sec^2\theta\right)\frac{\Delta\rho}{\rho}, \tag{16}$$

where $\Delta M/M$ is the P-wave modulus reflectivity, $\Delta\mu/\mu$ is the S-wave modulus reflectivity, and $\Delta\rho/\rho$ is the density reflectivity.

To examine the accuracy of our new Zoeppritz approximate equation 16, we compared it with the exact Zoeppritz equation. Figure 1a displays the reflection coefficient with the exact Zoeppritz equation (solid in red), Aki-Richards approximate equation (equation 10, thin solid in green), and the new approximate equation (dashed in black). The P-wave velocity, S-wave velocity, and density in the upper media are 2857 m/s, 1666 m/s, and 2275 kg/m^3, respectively, and in the lower media, they are 2898 m/s, 1290 m/s, and 2425 kg/m^3, respectively. Figure 1b displays the difference of the reflection coefficients from the exact Zoeppritz equation of the Aki-Richards approximate equation (solid in green) and of the new approximate equation (dashed in black). Figure 1c is a composite showing the synthetic common midpoint profile with the exact (red), Aki-Richards approximate equation (green), and the new approximate equation (black), all with the same Ricker wavelet. Note from Figure 1 that our new approximate approach is close to the modeling result from the exact Zoeppritz equation until the incident angle reaches 50°.

AVO INVERSION FOR P- AND S-WAVE MODULI

AVO inversion can be implemented with a Bayesian scheme (Buland and Omre, 2003). It can combine the observed data with any prior information. In this paper, we present a robust AVO inversion method with equation 16 and a convolution operation as the forward solver in the Bayesian paradigm. We chose a Cauchy probability distribution as the prior probability distribution because it can lead to a high resolution result (Sacchi and Ulrych, 1995; Theune et al., 2010). When there is a strong degree of correlation among the three parameters to be inverted, Alemie and Sacchi (2011) apply a Trivariate Cauchy distribution as prior information, and this not only leads to a high-resolution inversion result, but also incorporates the correlation. In this paper, we apply the Cauchy and an operator to decorrelate the parameters via the diagonalization of the covariance matrix. Furthermore, the low-frequency models from the well logs are incorporated into the objective function to enhance the stability and accuracy of the inversion.

The posterior probability distribution of the estimated model parameters in AVO inversion is expressed as the joint distribution of prior probability $p(\mathbf{m})$ and likelihood $p(\mathbf{d}|\mathbf{m})$ as follows:

$$p(\mathbf{m}|\mathbf{d}) = \frac{p(\mathbf{m})p(\mathbf{d}|\mathbf{m})}{\int p(\mathbf{d}|\mathbf{m})d\mathbf{m}} \propto p(\mathbf{m})p(\mathbf{d}|\mathbf{m}), \tag{17}$$

where $p(\bullet)$ means the probability density function, $\mathbf{m}$ means the parameter matrix to be inverted, namely, the P-wave modulus, S-wave modulus, and density reflectivity. Cauchy and Gaussian probability distributions for the prior probability distribution $p(\mathbf{m})$ and likelihood function $p(\mathbf{d}|\mathbf{m})$ are given as equations 18 and 19, respectively,

$$p(\mathbf{d}|\mathbf{m}) = \frac{1}{\sqrt{2\pi}\sigma_n} \exp\left[\frac{-(\mathbf{d}-\mathbf{Gm})^T(\mathbf{d}-\mathbf{Gm})}{2\sigma_n^2}\right], \tag{18}$$

$$p(\mathbf{m}) = \frac{1}{(\pi\sigma_m)^N} \prod_{i=1}^{N} \left[\frac{1}{1+m_i^2/\sigma_m^2}\right], \tag{19}$$

where σ_n^2 and σ_m^2 are the variance of the noise and model parameters, respectively, and $\mathbf{G}$ is a pseudo-wavelet matrix considering the decorrelation of the parameters to be inverted, while simultaneously containing the effect of incident angles and wavelet (Downton and Lines, 2004).

Substitute equations 18 and 19 into equation 17, and after some algebraic operation, the initial objective function for the maximum a posteriori solution inversion can be expressed as

$$F(\mathbf{m}) = (\mathbf{d}-G\mathbf{m})^T(\mathbf{d}-G\mathbf{m}) + 2\sigma_n^2 \sum_{i=1}^{M} \ln(1+m_i^2/\sigma_m^2). \tag{20}$$

Yin et al. (2008) add point constraints to enhance inversion stability. Here, we combine the low-frequency information constraint, which can be more easily estimated from well logging, with equation 20. Taking the low-frequency constraint on the P-wave modulus, for example, the relationship between P-wave modulus reflectivity matrix $\mathbf{M}_r$ and P-wave modulus matrix $\mathbf{M}$ is

$$\frac{1}{2}\ln\frac{\mathbf{M}(t)}{\mathbf{M}(t_0)} = \int_{t_0}^{t} \mathbf{M}_r(\tau)\mathrm{d}\tau. \tag{21}$$

Similarly,

$$\frac{1}{2}\ln\frac{\boldsymbol{\mu}(t)}{\boldsymbol{\mu}(t_0)} = \int_{t_0}^{t} \boldsymbol{\mu}_r(\tau)\mathrm{d}\tau, \tag{22}$$

$$\frac{1}{2}\ln\frac{\mathbf{D}(t)}{\mathbf{D}(t_0)} = \int_{t_0}^{t} \mathbf{D}_r(\tau)\mathrm{d}\tau, \tag{23}$$

where $\boldsymbol{\mu}_r$ and $\mathbf{D}_r$ are the S-wave modulus and density modulus reflectivity matrix, respectively; $\boldsymbol{\mu}$ and $\mathbf{D}$ are the S-wave modulus and density modulus matrix, respectively. Combining equation 21 with equation 23 into the initial objective function (found in equation 20), yields the final objective function,

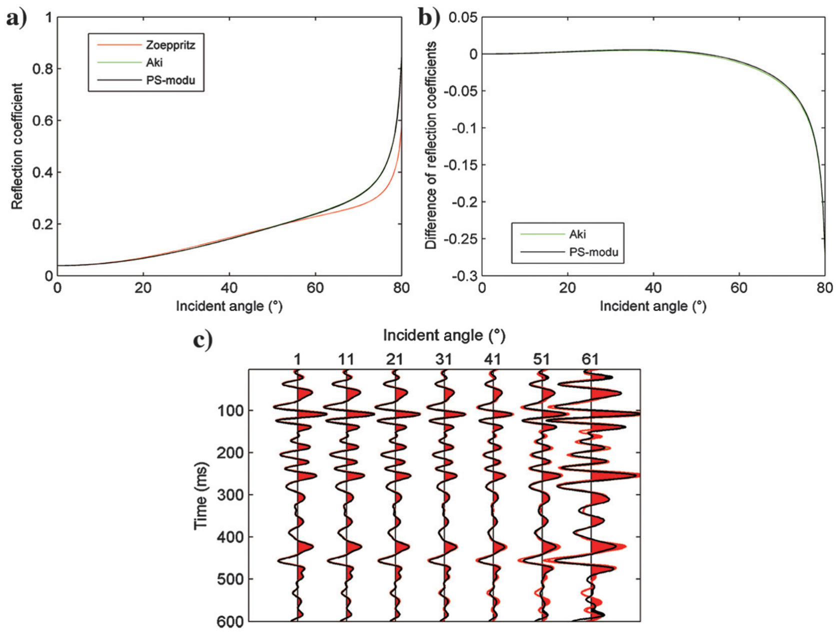

Figure 1. Comparison of the exact Zoeppritz equation, the Aki-Richards approximate equation, and the approximate equation in terms of P-wave modulus, S-wave modulus, and density. (a) Reflection coefficient with the exact Zoeppritz equation, the Aki-Richards approximate equation, and the approximate equation in terms of the P-wave modulus, S-wave modulus, and density. (b) Difference of reflection coefficients from the exact Zoeppritz equation, the Aki-Richards approximate equation, and the approximate equation in terms of the P-wave modulus, S-wave modulus, and density (c) Synthetic common midpoint profile with the exact Zoeppritz equation, the Aki-Richards approximate equation, and the approximate equation in terms of the P-wave modulus, S-wave modulus, and density with the same Ricker wavelet.

$$F(m) = (\mathbf{d} - \mathbf{Gm})^T(\mathbf{d} - \mathbf{Gm}) + 2\sigma_n^2 \sum_{i=1}^{M} \ln(1 + m_i^2/\sigma_{m_i}^2)$$
$$+ \lambda_M(\eta_M - \mathrm{P}\mathbf{M}_r)^T(\eta_M - \mathrm{P}\mathbf{M}_r)$$
$$+ \lambda_\mu(\eta_\mu - \mathrm{P}\boldsymbol{\mu}_r)^T(\eta_\mu - \mathrm{P}\boldsymbol{\mu}_r)$$
$$+ \lambda_D(\eta_D - \mathrm{P}\mathbf{D}_r)^T(\eta_D - \mathrm{P}\mathbf{D}_r), \tag{24}$$

where $\lambda_M, \lambda_\mu, \lambda_D$ are the constraint coefficients for the P-wave modulus, the S-wave modulus, and the density, P is $\int_{t_0}^{t} d\tau$, and

$$\eta_M = \frac{1}{2}\ln(\mathbf{M}/M_0), \tag{25}$$

$$\eta_M = 1/2 * \ln(\boldsymbol{\mu}/\mu_0), \tag{26}$$

$$\eta_M = 1/2 * \ln(\mathbf{D}/D_0), \tag{27}$$

where M_0, μ_0, and D_0 are the initial P-wave modulus, S-wave modulus, and density, which can be estimated from log curves. We solve equation 24 with the IRLS method (Daubechies et al., 2010). With only a few iterations, the algorithm can obtain reasonable convergence.

EXAMPLE RESULTS

Synthetic test

We test the inversion method on a synthetic earth profile with real well logs from well A. The seismic forward modeling is implemented using a convolution of the exact Zoeppritz equation with a Ricker wavelet, whose main frequency is 40 Hz, directly in the time-angle domain. Figure 2a, 2b, 2c, and 2d shows the synthetic common midpoint profile of well A with different S/N. S/N is the ratio between the root mean square amplitude of the signal and the root mean square amplitude of the noise, with the noise normally distributed. Figure 3a, 3b, 3c, and 3d shows the relevant original (in blue), initial (in green), and inverted (in red) P-wave modulus, S-wave modulus, and density curves, respectively, for four different S/Ns. The original moduli are from well logs, and they have been transformed from the depth domain to the time domain. The initial models are obtained by smoothing the original models. We perform the inversion with the novel approximate equation 16. From Figure 3a, we see that all the parameters can be inverted well when there is no noise in the synthetic data and with a rather smooth initial P-wave modulus, S-wave modulus, and density. To test the stability of the inversion method, we add random Gaussian noise to the synthetic traces, with different S/N, as displayed in Figure 3b, 3c, and 3d. The S/N is 2:1, 1:1, and 1:2, respectively. It is easy to demonstrate that the P- and S-wave moduli can be estimated reasonably even in the case with an S/N of 1:2 using the same smooth initial model as in the case with no noise, but the density does not fare as well.

Inversion of real data and fluid term calculation

An amplitude-preserving processing procedure was used for the real data to make sure final prestack amplitudes represent the reflection strength of the subsurface interfaces as nearly as possible. A small 3D field data set was used for inversion. We chose a CMP gather of one inline record with the known well at CMP 100 (we show just a few gathers) containing two effective oil reservoirs shown by the two yellow arrows in Figure 4. The gather is recorded in the time-offset domain, and we transform it to the time-angle domain prior to inversion; the maximum incident angle is around 30°. Figure 5a, 5b, and 5c shows the inverted P-wave modulus, S-wave modulus, and density, respectively, and the original and inverted curves at the well location are displayed in blue and red, respectively. We can see that the inverted P- and S-wave moduli, obtained with very smooth initial models, show good agreement with the known logs. The inverted density, however, shows uncertainty and departs significantly from the original density. With the reasonable inverted P- and S-wave moduli ii, we can easily use equation 9 to get the more credible fluid term profile displayed in Figure 6. Here c is 2.238 based on statistical analysis. For details of how to get c, refer to Russell et al. (2003). Two oil reservoirs can be clearly identified in the fluid term profile, and the fluid term calculated from the inverted P- and S-wave moduli shows good agreement with drilling results.

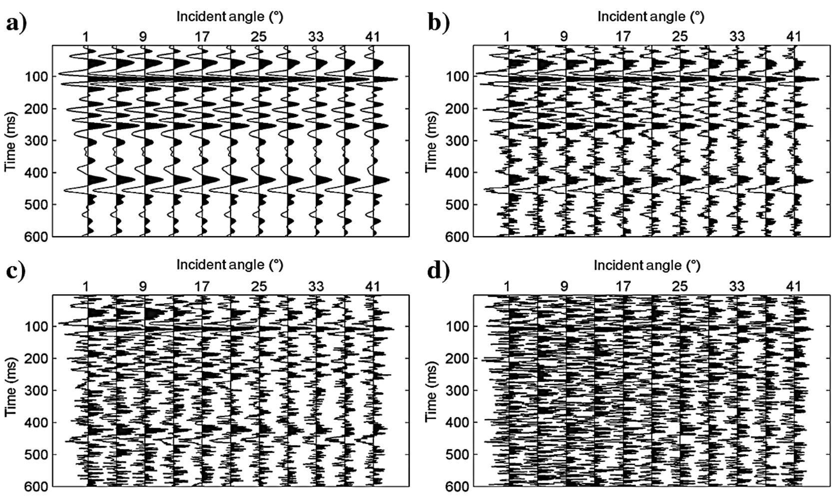

Figure 2. Synthetic trace with different S/N of well A: (a) no noise, (b) S/N = 2, (c) S/N = 1, (d) S/N = 1/2.

DISCUSSION

We used the poroelasticity theory to reformulate AVO inversion in terms of the P-wave modulus, S-wave modulus, and density. With this formulation, the fluid term f can be computed from the inverted compressional and shear moduli, without explicitly using the inverted density. The density is difficult to invert. Downton (2005) points out that large angles of incidence and large offsets are needed to determine density through AVO inversion. He also finds that the estimated density reflectivity shows more bias than the P- and S-impedance reflectivities when noise exists; i.e., the estimated density is more contaminated by noise than the estimated P- and S-impedance reflectivities, even with large incident angles. From Figure 3a, when there is no noise, the method presented here could well estimate the P-wave modulus, S-wave modulus, and density with a moderate maximum incident angle; however, the estimated density shows more bias when noise exists, as shown in Figure 3b, 3c, and 3d. From Figure 5c, we see that we could

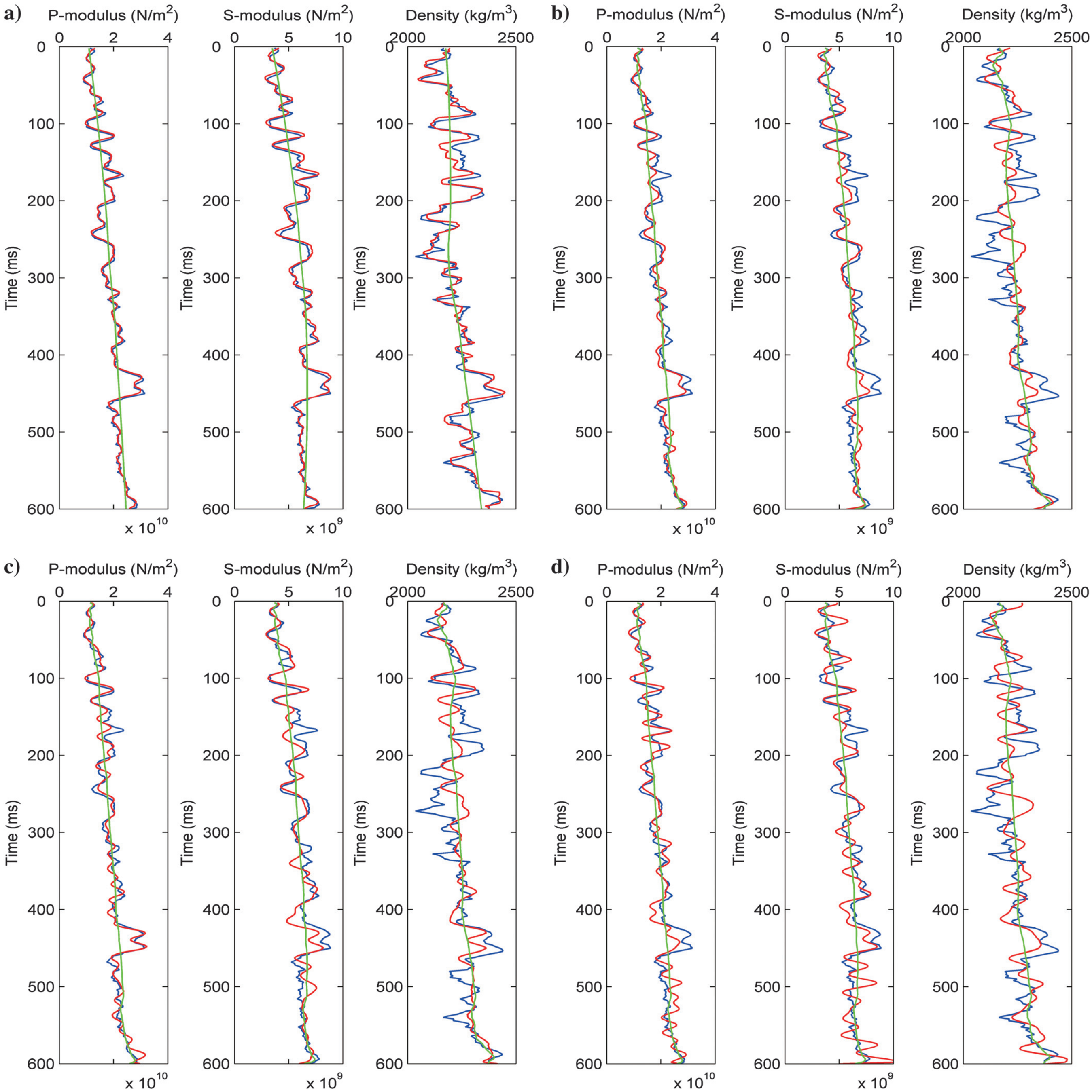

Figure 3. Model inversion result with different S/N (red is the inversion result, blue is the original model, and green is the initial model): (a) no noise, (b) $S/N = 2$, (c) $S/N = 1$, (d) $S/N = 1/2$.

not estimate a reasonable density profile because the maximum angle of incidence is only around 30°. Our formulation of the fluid response and AVO inversion gives the fluid term f in terms of the inverted products M and mu, without explicitly using the inverted density. We suggest that this formulation might minimize the effect of noise on the estimation of the fluid term f.

In addition to reformulating the poroelasticity theory and AVO inversion in terms of P- and S-wave moduli, we show that the approximate equation and fluid term f may also be expressed in terms of Lamé parameters, bulk modulus or Young's modulus, and so on. An approximate equation in term of the Lamé parameters (Goodway et al., 1997) lays the foundation for the following LMR technology, In practice, however, the physical meaning the first Lamé parameter λ is still controversial, and the Lamé parameter λ used to express P-wave velocity in isotropic, elastic nonporous, or porous media has no physical interpretation, but it serves to simplify the stiffness matrix in Hooke's law (Mavko et al., 1998).

CONCLUSIONS

In this paper, we introduced the P- and S-wave moduli into poroelasticity theory and AVO approximation, with which we presented a stable method to estimate the fluid term from prestack CMP seismic data. The introduction of P- and S-wave moduli into poroelasticity illustrated that we could get the fluid term f directly in theory, in a way that is meaningful and natural. The introduction of P- and S-wave moduli into the AVO approximation made it possible for the P- and S-wave moduli to be inverted directly from seismic data and also made the derivation of the AVO approximation combining poroelasticity and the AVO technology easy and meaningful. Compared with other indirect ways, such as those that invert the P-wave, S-wave impedances/velocities, and density simultaneously, our method does not need the density parameter, which is not easy to estimate due to the limits of geometry and noise levels in prestack data. Compared with direct inversion, this method can been seen as a helpful alternative approach to determine f from

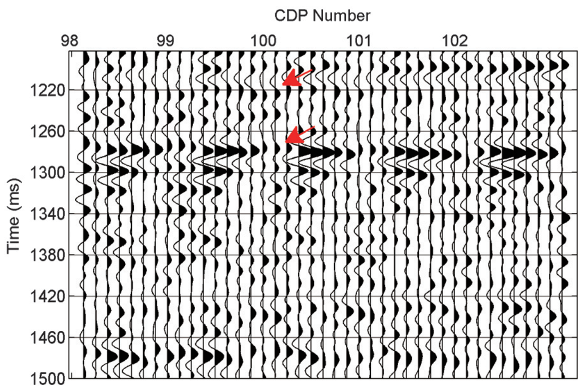

Figure 4. CMP gather of inline with the known well.

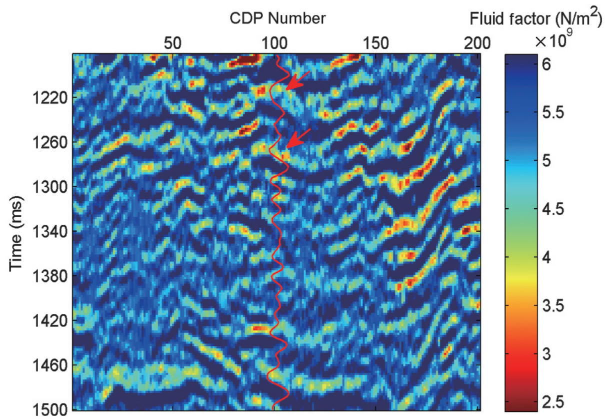

Figure 6. Fluid term of inline with the known well.

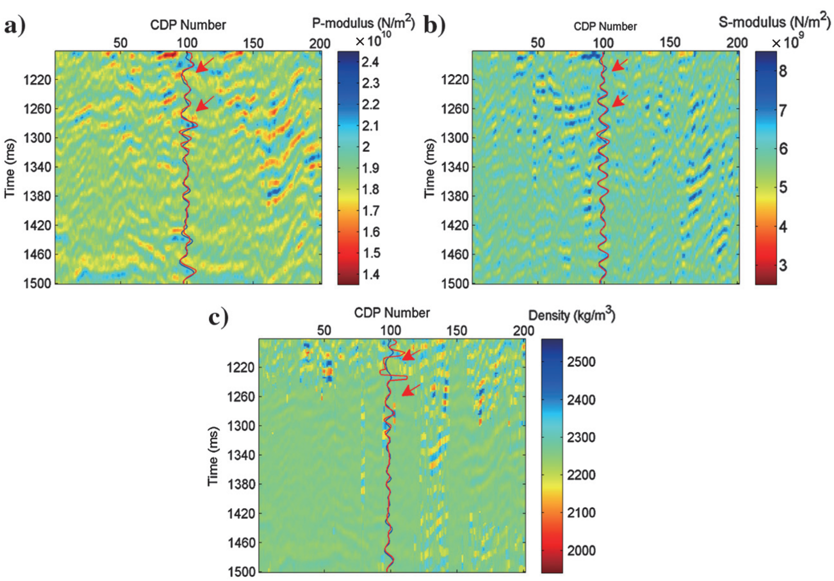

Figure 5. Profiles of inverted parameters with smooth initial models through the known well (a) P-wave modulus, (b) S-wave modulus, and (c) density.

prestack seismic data, especially in some cases in which $(V_S/V_P)^2_{dry}$ varies with depth.

We also presented a stable method to invert for P- and S-wave moduli based on our novel AVO approximate equation. The introduction of a low-frequency constraint and statistical probability information to the objective function renders the inversion more stable and less sensitive to the initial model. A synthetic test showed that this inversion method could obtain stable results for P- and S-wave moduli, starting from a very smooth initial model, even when the noise level is very high. It provided less reliable information about the density. The field test served to confirm the validity of the method, and it also showed that this fluid-term method for fluid discrimination could be applicable to oil reservoir identification.

ACKNOWLEDGMENTS

We would like to acknowledge the sponsorship of the National 973 Program of China (2013CB228604) and the National Grand Project for Science and Technology (2011ZX05030-004-002 and 2011ZX05019-003) for funding this research. We also thank the anonymous reviewers for their constructive suggestions.

REFERENCES

Aki, K., and P. G. Richards, 1980, Quantitative seismology (second ed.): W. H. Freeman and Co.

Alemie, W., and M. D. Sacchi, 2011, High-resolution three-term AVO inversion by means of a Trivariate Cauchy probability distribution: Geophysics, **76**, no. 3, R43–R55, doi: 10.1190/1.3554627.

Beretta, M. M., G. Bernasconi, and G. Drufuca, 2002, AVO and AVA inversion for fractured reservoir characterization: Geophysics, **67**, 300–306, doi: 10.1190/1.1451802.

Biot, M., 1956, General solutions of the equations of elasticity and consolidation for a porous material: Journal of Applied Mechanics, **23**, 91–96.

Biot, M. A., 1941, General theory of three dimensional consolidation: Journal of Applied Physics, **12**, 155–164, doi: 10.1063/1.1712886.

Buland, A., and M. Landro, 1995, AVO inversion, theory and applications: Journal of Applied Geophysics, **34**, 140–140, doi: 10.1016/0926-9851(96)80869-X.

Buland, A., and H. Omre, 2003, Bayesian linearized AVO inversion: Geophysics, **68**, 185–198, doi: 10.1190/1.1543206.

Daubechies, I., R. DeVore, M. Fornasier, and C. S. Güntürk, 2010, Iteratively reweighted least squares minimization for sparse recovery: Communications on Pure and Applied Mathematics, **63**, 1–38, doi: 10.1002/cpa.v63:1.

Downton, J. E., 2005, Seismic parameter estimation from AVO inversion: Ph.D. thesis, University of Calgary.

Downton, J. E., and L. R. Lines, 2004, Three term AVO waveform inversion: 74th Annual International Meeting, SEG, Expanded Abstracts, 215–218.

Downton, J. E., and C. Ursenbach, 2006, Linearized amplitude variation with offset (AVO) inversion with supercritical angles: Geophysics, **71**, no. 5, E49–E55, doi: 10.1190/1.2227617.

Garat, J., M. Krief, J. Stellingwerff, and J. Ventre, 1990, A petrophysical interpretation using the velocities of P and S waves (full-waveform sonic): Log Analyst, **31**, 355–369.

Gassmann, F., 1951, Über die Elastizität poröser Medien: Vierteljahrsschrift der Naturforschenden Gesellschaft in Zurich, **96**, 1–23.

Goodway, B., T. Chen, and J. Downton, 1997, Improved AVO fluid detection and lithology discrimination using Lamé petrophysical parameters; "$\lambda\rho$", "$\mu\rho$", & "λ/μ fluid stack", from P and S inversions: 67th Annual International Meeting, SEG, Expanded Abstracts, 183–186.

Ikelle, L. T., 1995, Linearized inversion of 3-D multi-offset data: Background reconstruction and AVO inversion: Geophysical Journal International, **123**, 507–528, doi: 10.1111/gji.1995.123.issue-2.

Jin, S., G. Cambois, and C. Vuillermoz, 2000, Shear-wave velocity and density estimation from *PS*-wave AVO analysis: Application to an OBS dataset from the North Sea: Geophysics, **65**, 1446–1454, doi: 10.1190/1.1444833.

Karimi, O., H. Omre, M. Mohammadzadeh, and S. Singleton, 2010, Bayesian closed-skew Gaussian inversion of seismic AVO data for elastic material properties: Geophysics, **75**, no. 1, R1–R11, doi: 10.1190/1.3299291.

Mavko, G., T. Mukerji, and J. Dvorkin, 1998, The rock physics handbook: Tools for seismic analysis in porous media: Cambridge University Press, 329.

Quakenbush, M., B. Shang, and C. Tuttle, 2006, Poisson impedance: The Leading Edge, **25**, 128–138, doi: 10.1190/1.2172301.

Russell, B. H., D. Gray, and D. P. Hampson, 2011, Linearized AVO and poroelasticity: Geophysics, **76**, no. 3, C19–C29, doi: 10.1190/1.3555082.

Russell, B. H., K. Hedlin, F. J. Hilterman, and L. R. Lines, 2003, Fluid-property discrimination with AVO: A Biot-Gassmann perspective: Geophysics, **68**, 29–39, doi: 10.1190/1.1543192.

Sacchi, M. D., and T. J. Ulrych, 1995, High-resolution velocity gathers and offset space reconstruction: Geophysics, **60**, 1169–1177, doi: 10.1190/1.1443845.

Simmons, J. L., and M. M. Backus, 1996, Waveform-based AVO inversion and AVO prediction-error: Geophysics, **61**, 1575–1588, doi: 10.1190/1.1444077.

Smith, G. C., and M. Gidlow, 2000, A comparison of the fluid factor with lambda and mu in AVO analysis: 70th Annual International Meeting, SEG, Expanded Abstracts, 122–125.

Smith, G. C., and P. M. Gidlow, 1987, Weighted stacking for rock property estimation and detection of gas: Geophysical Prospecting, **35**, 993–1014, doi: 10.1111/gpr.1987.35.issue-9.

Theune, U., I. Ø. Jensas, and J. Eidsvik, 2010, Analysis of prior models for a blocky inversion of seismic AVA data: Geophysics, **75**, no. 3, C25–C35, doi: 10.1190/1.3427538.

Yin, X., P. Yang, and G. Zhang, 2008, A novel prestack AVO inversion and its application: 78th Annual International Meeting, SEG, Expanded Abstracts, 2041–2045.

Zoeppritz, K., 1919, Erdbebenwellen VIII B, Uber die Reflexion und Durchgang seismischer Wellen durch Unstetigkeitsflachen: Gottinger Nachr, **1**, 66–84.